Report

Keeping up with Bats: Dynamic Auditory Tuning in a Moth

James Frederick Charles Windmill,[1,*]
Joseph Curt Jackson,[1] Elizabeth Jane Tuck,[1]
and Daniel Robert[1]
[1] School of Biological Sciences
University of Bristol
Woodland Road
Bristol BS8 1UG
United Kingdom

Summary

Many night-flying insects evolved ultrasound sensitive ears in response to acoustic predation by echolocating bats [1–10]. Noctuid moths are most sensitive to frequencies at 20–40 kHz [6], the lower range of bat ultrasound [5, 11–13]. This may disadvantage the moth because noctuid-hunting bats in particular echolocate at higher frequencies shortly before prey capture [7, 11–13] and thus improve their echolocation and reduce their acoustic conspicuousness [6–10, 12–16]. Yet, moth hearing is not simple; the ear's nonlinear dynamic response shifts its mechanical sensitivity up to high frequencies. Dependent on incident sound intensity, the moth's ear mechanically tunes up and anticipates the high frequencies used by hunting bats. Surprisingly, this tuning is hysteretic, keeping the ear tuned up for the bat's possible return. A mathematical model is constructed for predicting a linear relationship between the ear's mechanical stiffness and sound intensity. This nonlinear mechanical response is a parametric amplitude dependence [17, 18] that may constitute a feature common to other sensory systems. Adding another twist to the coevolutionary arms race between moths and bats, these results reveal unexpected sophistication in one of the simplest ears known and a novel perspective for interpreting bat echolocation calls.

Results and Discussion

Bat echolocation calls have a sophisticated acoustic structure, yet they tend to follow a predictable temporal sequence [5, 7, 8, 11]. From the acoustic perspective of a moth, as an aerial-hunting bat approaches, the incident amplitude of the call increases and its duration shortens [7, 11, 14, 16]. Concurrently, the frequency bandwidth dramatically increases, a spectral broadening that refines the accuracy of the bat's biosonar [6, 7]. To the moth, these variations could be a telltale sign that the bat is homing in on its prey [7, 14]. Yet, moth ears are anatomically simple. The ears of the noctuid moths studied here are endowed with only three mechanosensory neurones (two auditory A cells with similar frequency tuning and one stretch-sensitive B

cell whose function is unclear) [2, 6]. These ears are generally considered to be tone-deaf [6, 9] and therefore seem only partially adapted to detect bat calls.

In light of the somewhat puzzling mistuning between moth hearing and bat calls, we set out to investigate the mechanical response of moth ears in the presence of simulated, yet realistic, bat calls. The noctuid moth *Noctua pronuba*, the large yellow underwing, was chosen because it is a sizable and abundant prey item for a large variety of echolocating bats (Figure 1A). The mechanical sensitivity of the moth's ear to bat sounds was investigated with microscanning laser Doppler vibrometry, a highly sensitive (10 pm amplitude resolution) noncontact and nonloading optical technique (see the Experimental Procedures). Although the moths were immobilized firmly so that stable optical measurements could be achieved, particular care was taken so that their nervous systems were not injured.

When stimulated with a series of pure tone pulses, the vibrational response of the moth tympanum is conspicuously nonlinear. The regular delivery of identical sound pulses results in tympanal vibrations of varying amplitude (Figure 1B). Physically, a simple harmonic oscillator (SHO), such as the membrane of a drum, cannot undergo such a response. The observed amplitude modulation points to a slow, nonlinear alteration of the mechanical properties of the moth's auditory system. The tympanal response was also measured in the frequency domain, with frequency-sweep stimulation (20–80 kHz; 80 ms duration), delivered at two different sound pressures: $f_{0,l}$ = 20 dB SPL and $f_{0,h}$ = 55 dB SPL (Figure 1C). Quite surprisingly, as sound pressure increased, the resonant frequency tuning of the moth ear shifted toward higher frequencies. The resonant peaks were $f_{0,l}$ = 42 kHz for low intensity and $f_{0,h}$ = 74 kHz for high intensity; the related phase at zero crossing shifted accordingly (Figure 1C, green and orange curves). This change in tuning failed to take place in dead, control animals (Figure 1C, gray ghost curve) and those under CO_2 hypoxia (data not shown).

Because moth hearing is the product of evolutionary adaptation to bat predation, a pertinent experiment was to document the time-resolved mechanics of moth hearing in response to bat-like acoustic signals. As a bat searches for, detects, and approaches its target, its echolocation calls change; pulse duration shortens whereas the spectral composition widens to include higher frequencies (Figure 2A, inset) [7, 10, 13]. For separation of frequency from both amplitude and duration effects, a series of four bat-like stimuli were synthesized with a constant carrier frequency of 30 kHz but with different amplitudes and temporal features. For simplicity, two biologically relevant amplitudes of 73 and 87 dB (SPL re. 20 μPa) and two temporal regimes with a bat-like duty cycle of 5% were chosen. One stimulus consisted of a train of 5 ms sound pulses every 100 ms (slow repetition rate of 10 Hz) and thus mimicked a distant bat in search of prey; the other stimulus carried
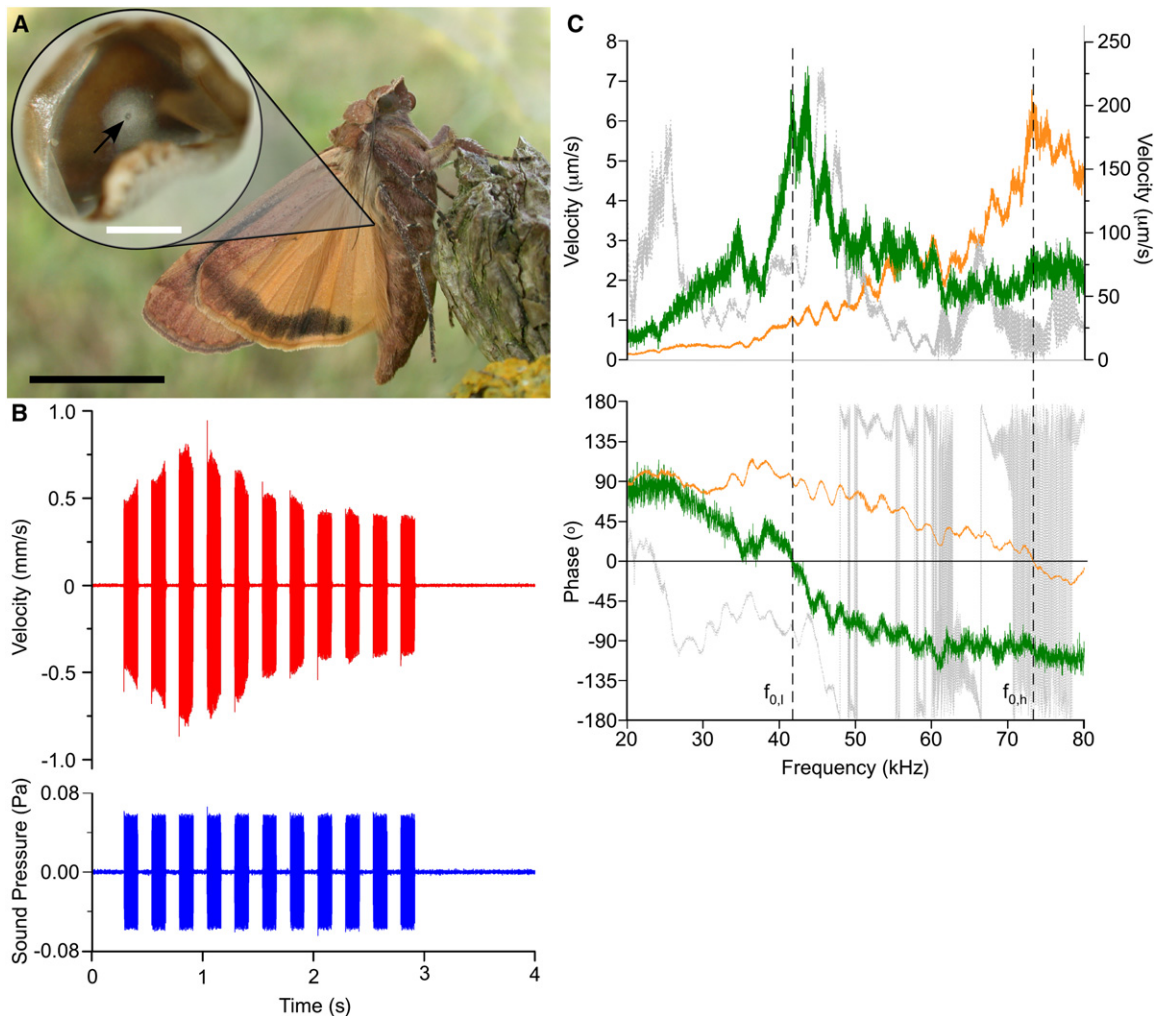
*Correspondence: james.windmill@bristol.ac.uk

Figure 1. Tympanal Vibrations in the Moth *Noctua pronuba* Are Time and Amplitude Dependent

(A) *N. pronuba* and a light micrograph of its microscale ear. The attachment site of the mechanosensory cells is visible (black dot; arrowhead in inset) near the center of the tympanal membrane (scale bars represent 1 mm, inset: 300 μm).

(B) Time-resolved mechanical response (red trace) of the moth tympanal membrane to bat-like sounds (blue trace) (125 ms pulse duration, 30 kHz tone, 70 dB SPL).

(C) Frequency spectrum of the mechanical response in magnitude (top panel) and phase (bottom panel). The response was measured in response to frequency-sweep stimulation (20–80 kHz, 80 ms). The green curve depicts the response to stimulation at low stimulus intensity (left ordinate), the orange curve depicts the response at high stimulus intensity (+35 dB) (right ordinate). The gray ghost curve is the response to stimulation with high sound level when the animal is dead. The zero crossing of the phase response (bottom panel) constitutes an accurate measure for the resonant frequency of the oscillator $f_{0,l}$ for the low-intensity stimulus and $f_{0,h}$ for the high-intensity stimulus.

short 0.5 ms pulses every 10 ms (fast repetition rate of 100 Hz) and was thus indicative of a bat looming onto its prey. The time-resolved responses reveal dramatic and unexpected changes in tympanal mechanics (Figure 2A). For either temporal regime (10 or 100 Hz repetition rate), at high sound level (87 dB SPL; equivalent to a bat ∼3 m away [19]), the moth's ear tunes up to high frequencies (70–80 kHz) within 0.75 s. For a stimulus with lower sound level (73 dB SPL; bat is ∼10 m away), the tympanum tunes up within ∼6 s. The results show that tuning up strongly depends on stimulus amplitude rather than stimulus repetition rate. Notably, this response was never observed in freshly decapitated moths (n = 10). The time-resolved phase data also indicate that the change in resonant frequency begins ∼105 ms (SD = 58.2, n = 10) after stimulus onset. These

results are unusual for an auditory system. Not only does frequency of best hearing change with stimulus amplitude, but tuning to high frequencies can take place irrespective of the spectral composition of the stimulus.

Another unexpected but salient feature of the moth's tympanal mechanics is tuning hysteresis accompanied by relaxation. Whereas the tympanum resonant frequency can be quickly or gradually brought up by an increased sound-pressure level (Figure 2B), its return to the low frequency state is slow. This tuning is highly hysteretic; reducing sound level by 20 dB does not immediately affect the high-frequency resonance (Figure 2B; black diamond). We characterized the duration and shape of hysteresis by probing tympanal tuning at regular 30 s intervals with low-intensity frequency sweeps that alone do not elicit high-resonance tuning. Hysteresis lasted
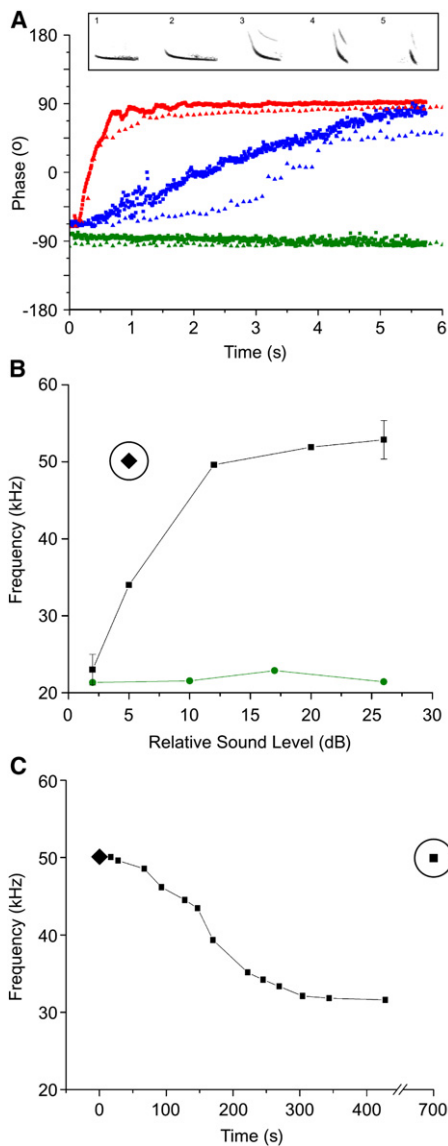
Figure 2. Amplitude-Dependent Frequency Tuning and Hysteretic Response to Bat-like Sounds

(A) The time-resolved phase response. Phase values were calculated from analytic signals constructed via Hilbert transforms. The top panel shows sonograms of bat calls at different stages of the approach (data from [16]). Triangles represent amplitude-dependent response to a "search" stimulus of 5 ms pulses, repeated every 100 ms. Squares represent response to a more urgent "approach" stimulus of 0.5 ms pulses, repeated every 10 ms. Both short and long pulse regimes are tested for two different sound levels (blue: 73 dB SPL, red: 87 dB SPL). A single frequency was used (30 kHz) for accurate and reliable measurement of resonant frequency tuning (Figure 1B). As for a broadband stimulus (as in Figure 1C), 30 kHz pulses elicit a phase change revealing tuning up to higher frequencies. No such change could be observed for any stimulus regimes in decapitated moths (green data).

(B) Quantitative amplitude dependence and hysteresis. The tympanum's resonant frequency gradually increases with stimulus amplitude (stimulus as in Figure 1C). Resonant frequency increases, on average, to 54 kHz (SD = 8.75, n = 16, range: 37.2–72.3 kHz), from 33 kHz (SD = 9.7, n = 16, range: 20–49.8 kHz). Error bars are defined as the SE. The response is highly hysteretic; acoustic stimulation attenuated by 20 dB (black diamond) elicits a high-frequency resonance (50.1 kHz). Post mortem, there is no change in the frequency response with amplitude and hence no hysteresis (green data).

for several minutes, during which a slow relaxation returned the tympanum to its low resonant frequency (Figure 2C). Interestingly, once the system has returned to its low-frequency state, a single high-amplitude pulse (pure tone or broadband sweep) restores the high-frequency tuning state (Figure 2C). This test indicates that relaxation cannot be due to a physiological deterioration of the auditory system.

To gain more insight into the mechanisms responsible for frequency tuning, we developed a model that accounts for the observed changes. The key working hypothesis is that the variation in the resonant frequency is due to a change in the stiffness of the system. This hypothesis is reasonable because a nonlinear, amplitude-dependent change in resonance has been previously documented in the auditory system of the fruit fly Drosophila [20] and in vertebrate hair cells [21]. Basing the system on an SHO, we then aimed at introducing such a nonlinearity. For an SHO with stiffness k and mass m, the natural frequency obeys $\omega_0 = \sqrt{k/m}$. As motivated by the experimental evidence, the natural resonant frequency is not constant but, for this new oscillator, depends on vibration amplitude $X = X(t)$. Formally, this is equivalent to introducing an additional stiffness $s(X)$ such that the effective resonant frequency ω_{eff} obeys:

$$\omega_{eff}^2 = \frac{k + s(X)}{m} = \omega_0^2 + \frac{s(X)}{m} \qquad (1)$$

The nature of the dependence of stiffness on amplitude, $s(X)$ is crucial. Guided by our experimental data, we utilized the simple relation:

$$\frac{ds(t)}{dt} = \frac{1}{\tau}(pX^\alpha - s(t)) \qquad (2)$$

where τ is a characteristic decay time and α and p are constants corresponding to the strength of the dependence. Equation 2 governs the dynamic behavior of the auditory system's stiffness as the vibration amplitude X changes. When applying a constant stimulus, Equation 2 indicates that, in the steady state, stiffness s_0 is related to the equilibrium amplitude X_0, by the equation $s_0 = pX_0^\alpha$. The time taken for the system to arrive at the steady state is governed by the time constant τ, a value that is commensurate with the dynamics of the stiffness change, on the order of seconds. Important in this formalism is the constant α, which describes the strength of the nonlinearity and is fundamental to modelling the process that endows the moth with amplitude-dependent tuning. Hence, the strength of the relationship between amplitude and stiffness is modeled by a power-law dependency. The power law can be determined from the convergence to a straight line log-log relationship between sound pressure and vibration

(C) Time-resolved characterization of the hysteretic response. Starting from a tuned-up state (diamond from (B) is now at time zero), the tympanum's resonant frequency returns to low-frequency tuning within 7.5 min. We measured slow relaxation by probing the mechanical response at 30 s intervals with a low-amplitude frequency-sweep stimulus (as in Figure 1C). After 7.5 min, a similar probe signal, but louder by 20 dB, could elicit again the high-frequency resonance.
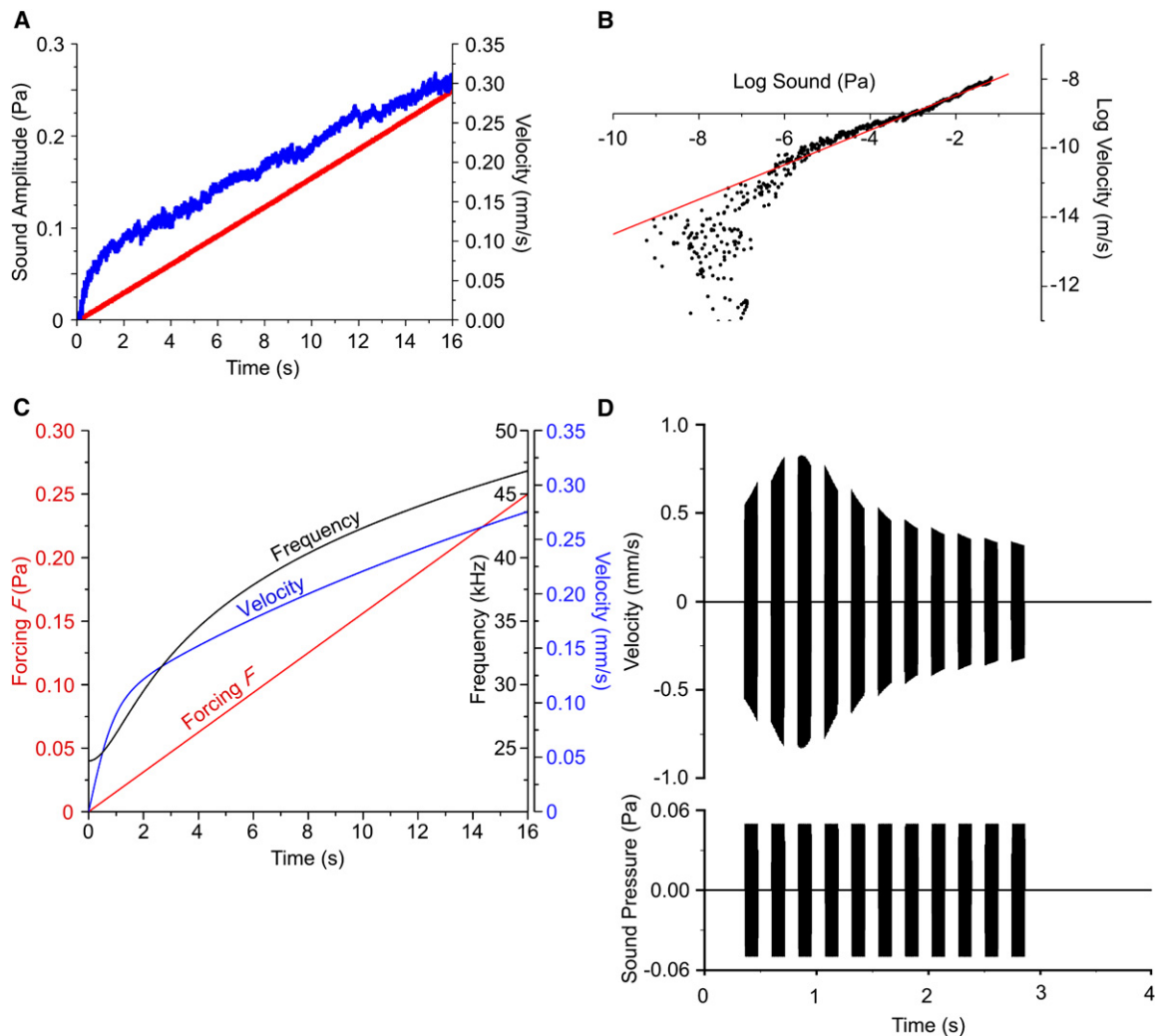
Figure 3. Modelling the Nonlinear Response of the Moth's Ear

(A) Experimental vibration velocity of the tympanal membrane (blue) in response to a continuously increasing sound amplitude (red), from ~0 to 82 dB SPL (30 kHz sine-wave stimulus). The nonlinear nature of the tympanal mechanical system is apparent from the deviation in velocity observed.

(B) Experimental relation between vibration velocity and forcing amplitude as a log-log plot. The slope of that relation converges to 0.5. This power law implies the existence of a linear relationship between the stiffness of the resonating system and the sound amplitude in the regime studied. Each data point is obtained from the discretization of the amplitude function into 4.88 μs intervals.

(C) Model-response characteristics of the nonlinear amplitude and frequency responses. The model's time-resolved behavior is tested in response to a continuously increasing amplitude forcing F (red; as in [A]).

(D) Time-resolved velocity response of the model system in response to bat-like sound pulses (125 ms duration, 30 kHz carrier frequency). The model response accurately mimics the response of the moth ear (Figure 1B).

velocity of the oscillator, noting that for a stimulus of amplitude F, as $F \rightarrow \infty$, $X \propto F^{\frac{1}{\alpha+1}}$ (see the Experimental Procedures in the Supplemental Data available with this article online). A sinusoidal stimulus with a slowly increasing amplitude was applied first so that the response of the tympanal system to increased F could be measured (Figure 3A). The power law was experimentally determined (Figure 3B) to be 0.5, which gives $\alpha \approx 1$ and thus implies a linear dependence between stiffness and amplitude. Applying a ramped amplitude stimulus to the model (as in Figure 3A) produces an output that corroborates the behavior of the moth's ear. Both resonant frequency and tympanal vibrations increase with forcing level F (Figure 3C). To further test the model, we applied a stimulus regime identical to

that used in Figure 1B. Remarkably, the model output mimics, in great detail, the nonlinear amplitude profile of the tympanal response (Figure 3D). This suggests that the dynamic changes observed in the response are caused by an amplitude-dependent change in the system's stiffness. Also, the convergence to a power law in the experimental data signifies that the proposed formalism is correct in the regime studied.

The model proposed is now useful in several ways. It predicts a testable linear relationship between the tympanal system's stiffness and its vibration amplitude, suggesting a series of experiments aiming at determining the dynamic, frequency-dependent Young's modulus of the entire system, and in particular that of the sensory neurones. Further, the model is designed for

providing time resolved predictions, with measurable physical parameters that could be unambiguously compared to physiological and mechanical data acquired in the time domain. The fact that tuning up ceases when the system is physiologically compromised points to an active auditory mechanism [22–24] possibly related to those reported for other insects, such as mosquitoes [22] and *Drosophila* [20]. Thus far, in insects, nonlinearities have been causally linked to the functional participation of mechanoreceptor cells; retuning of the moth ear may well be the consequence of such cellular involvement. In this sense, unlike a cochlear amplifier [23], the moth ear operates to tune rather than amplify. A prime suspect for the role of "active tuner" cell is the B cell with its elusive function. This cell has been reported to slowly vary its firing activity, with sound intensity in one study using intact moths [25] or with proprioceptive input [26]. Moths and bats share the night sky and a convoluted coevolutionary relationship; by listening for bat calls in the dark, moths have developed the capacity to not only detect hunting bats but also to get a sense of whether the bat may be aware of their presence. In turn, whether bats are able to modify their echolocation behavior in response to such active tuning constitutes an outstanding and fascinating question.

Experimental Procedures

Animals and Experimental Setup
Male and female *Noctua pronuba* were captured at Leigh Woods nature reserve, near Bristol (UK). After 10 p.m., moth traps were set up, with vertical white cotton sheets illuminated by ultraviolet fluorescent and halogen lamps. Individuals were placed into mesh cages (30 × 30 × 45 cm) and supplied with 5% sugar water. Moths were always used within 24 hr after capture. The vibrometry measurements required for one of the animal's wings to be slightly cut back to allow optical access to the tympanal ears. The moth was firmly attached, ventrum down, to an adjustable, horizontal, and electrically grounded brass bar (10 mm long, 5 mm wide, 1 mm thick) with low-melting-point paraffin wax. Only one ear was examined per animal. For the decapitation experiments, measurements were carried out less than a minute after surgery. The moth was orientated such that the measuring laser Doppler vibrometer could access the entire tympanal membrane, and that the tympanum was perpendicular to the direction of sound propagation. All experiments were carried out on a vibration isolation table (TMC 784-443-12R) at room temperature (24°C–26°C) and relative humidity of 40%–62%. The vibration isolation table and the laser vibrometry measurement head were located in an acoustic isolation booth resting on rubber dampers (Industrial Acoustics IAC series 1204A, internal dimensions: length = 4.50 m, width = 2.25 m, height = 1.98 m).

Mechanical and Acoustic Measurements
All vibration analyses required the simultaneous recording of the vibration velocity of the tympanal membrane and the local sound-pressure level. Tympanal vibrations were measured with a micro-scanning laser Doppler vibrometer (Polytec PSV-300-F) with an OFV-056 scanning head fitted with a 150 mm lens. This allowed the laser spot ($\sim$5 μm diameter) to be positioned with an accuracy of $\sim$1 μm. Low noise and high spatial-resolution measurements could be taken at any point on the tympanal membrane without readjusting the position of the animal in the sound field or any component in the setup. The exact location of the laser beam on the tympanum was monitored via a live video camera coaxial with the laser's optical axis. Thus, there was a constant certainty that measurements were always taken on the point of attachment of the sensory neurones to the tympanal membrane. Vibrations could be measured with a resolution of 10 pm in the amplitude domain, without mechanical contact or loading and without requiring the use of a reflective medium.

Tympanal vibrations were characterized in response to various acoustic stimuli. First, wideband frequency sweeps were used ranging 20–80 kHz. The acoustic signals were generated by the PSV 300's internal data acquisition board (National Instruments PCI-4451), passed through a JFW Industries attenuator, and amplified (Sony Amplifier Model TA-FE570) to be finally delivered by a high-temporal-fidelity loudspeaker (Sony SACD SS-TW11ED supertweeter) positioned 300 mm from the animal. For the relevant frequency range (20–80 kHz), the animal was in the far field of the sound source. Sound pressure was measured with a 1/8″ (3.2 mm) precision pressure microphone (Bruel and Kjaer, 4138) and preamplifier (Bruel and Kjaer, 2633). This reference microphone has a linear response in the measured frequency and amplitude ranges. The microphone's sensitivity was calibrated with a Bruel and Kjaer sound-level calibrator (4231, calibration at 1 kHz, 94 dB SPL). The microphone was positioned 5 mm from the moth's tympanum, with its diaphragm parallel to the direction of sound propagation, thus maximizing the microphone's amplitude accuracy. The acoustic signals were digitally synthesized for ensuring that stimulus amplitude was kept to a constant level across the entire frequency spectrum (20–80 kHz). To achieve this, we measured the incident sound-frequency spectrum, as sensed by the reference microphone, in signal voltage and inverted it with respect to amplitude. We fed the resulting voltage-frequency function (inverse spectrum) back to the waveform generator to create a corrected spectrum in order to flatten the amplitude distribution of the stimulus at the position of the reference microphone. Between 20 and 80 kHz, stimulus amplitude varied by, in SD, ±0.99 dB and ±7.82 dB for sound pressures of 50 and 80 dB SPL, respectively.

Data Analysis
The analysis of membrane velocity and sound pressure was carried out with a combination of Polytec v.7.4 software and National Instruments LabVIEW v.8.0. Both vibrometer and reference microphone signals were simultaneously sampled at 204.8 kHz. Sets of 25 data windows of 80 ms duration were acquired and averaged for each measurement on the tympanal membrane. With a Fast Fourier Transform with a rectangular window (for accurate frequency estimate), amplitude and phase frequency spectra were produced with a resolution of 12.5 Hz. Time-domain phase data was calculated by Hilbert transforms with LabVIEW. The magnitude-squared coherence between the vibrometer and microphone signals was also computed for each data point so that data quality for the entire data set could be assessed. Data was considered of sufficient quality when coherence exceeded 85%.

Supplemental Data
Supplemental Data include additional Experimental Procedures and can be found with this article online at http://www.current-biology.com/cgi/content/full/16/24/2418/DC1/.

References

1. Griffin, D.R. (1958). Listening in the Dark: The Acoustic Orientation of Bats and Men (New Haven, CT: Yale University Press).
2. Roeder, K.D. (1967). Nerve Cells and Behavior (Cambridge, MA: Harvard University Press).

3. Roeder, K.D., and Treat, A.E. (1957). Ultrasonic reception by the tympanic organ of noctuid moths. J. Exp. Zool. *134*, 127–157.

4. Griffin, D.R. (1953). Bat sounds under natural conditions, with evidence for echolocation of insect prey. J. Exp. Zool. *123*, 435–465.

5. Jones, G. (2005). Echolocation. Curr. Biol. *15*, 484–488.

6. Fullard, J.H. (1988). The tuning of moth ears. Experientia *44*, 423–428.

7. Fullard, J.H., Dawson, J.W., and Jacobs, D.S. (2003). Auditory encoding during the last moment of a moth's life. J. Exp. Biol. *206*, 281–294.

8. Waters, D.A., and Jones, G. (1996). The peripheral auditory characteristics of noctuid moths: Responses to the search-phase echolocation calls of bats. J. Exp. Biol. *199*, 847–856.

9. Yack, J.E. (2004). The structure and function of auditory chordotonal organs in insects. Microscopy Research and Technique *63*, 315–337.

10. Yack, J.E., and Fullard, J.H. (2000). Ultrasonic hearing in nocturnal butterflies. Nature *403*, 265–266.

11. Surlykke, A., and Moss, C.F. (2000). Echolocation behavior of big brown bats, Eptesicus fuscus, in the field and the laboratory. J. Acoust. Soc. Am. *108*, 2419–2429.

12. Kingston, T., and Rossiter, S.J. (2004). Harmonic hopping in Wallacea's bats. Nature *429*, 654–657.

13. Siemers, B.M., and Schnitzler, H.-U. (2004). Echolocation signals reflect niche differentiation in five sympatric congeneric bat species. Nature *429*, 657–661.

14. Faure, P.A., Fullard, J.H., and Dawson, J.W. (1993). The gleaning attacks of the northern long-eared bat, Myotis Septentrionalis, are relatively inaudible to moths. J. Exp. Biol. *178*, 173–189.

15. Waters, D.A. (2003). Bats and moths: What is there left to learn? Physiological Entomology *28*, 237–250.

16. Holderied, M.W., Korine, C., Fenton, M.B., Parsons, S., Robson, S., and Jones, G. (2005). Echolocation call intensity in the aerial hawking bat Eptesicus bottae (Vespertilionidae) studied using stereo videogrammetry. J. Exp. Biol. *208*, 1321–1327.

17. Pikovsky, A., Rosenblum, M., and Kurths, J. (2001). Synchronization: A Universal Concept in Nonlinear Sciences (Cambridge: Cambridge University Press).

18. Strogatz, S.H. (2000). Nonlinear Dynamics and Chaos (Cambridge, MA: Perseus).

19. Lawrence, B.D., and Simmons, J.A. (1982). Measurements of atmospheric attenuation at ultrasonic frequencies and the significance for echolocation by bats. J. Acoust. Soc. Am. *71*, 585–590.

20. Göpfert, M.C., and Robert, D. (2003). Motion generation by Drosophila mechanosensory neurons. Proc. Natl. Acad. Sci. USA *100*, 5514–5551.

21. Martin, P., Mehta, A.D., and Hudspeth, A.J. (2000). Negative hair-bundle stiffness betrays a mechanism for mechanical amplification by the hair cell. Proc. Natl. Acad. Sci. USA *97*, 12026–12031.

22. Göpfert, M.C., and Robert, D. (2001). Active auditory mechanics in mosquitoes. Proc. R. Soc. Lond. B. Biol. Sci. *268*, 333–339.

23. Hudspeth, A.J. (1997). Mechanical amplification by hair cells. Curr. Opin. Neurobiol. *7*, 480–486.

24. Robert, D., and Göpfert, M.C. (2002). Novel schemes for hearing and acoustic orientation in insects. Curr. Opin. Neurobiol. *12*, 715–720.

25. Lechtenberg, R. (1971). Acoustic response of B-cell in Noctuid moths. Journal of Insect Physiology *17*, 2395–2399.

26. Yack, J.E. (1992). A multiterminal stretch receptor, chordotonal organ, and hair plate at the wing-hinge of Manduca sexta: Unravelling the mystery of the noctuid moth ear B cell. J. Comp. Neurol. *324*, 500–508.